ELSEVIER

Polymer 42 (2001) 7819–7830

polymer

www.elsevier.nl/locate/polymer

Miscibility of ethylene–styrene copolymer blends

H.Y. Chen[a], Y.W. Cheung[b], A. Hiltner[a,*], E. Baer[a]

[a]*Department of Macromolecular Science, Center for Applied Polymer Research, Case Western Reserve University, Kent Hale Smith Bldg. Rm. 423, 10900 Euclid Ave., Cleveland, OH 44106-7202, USA*

[b]*Polyolefins and Elastomers R & D, The Dow Chemical Company, Freeport, TX 77541, USA*

Received 7 November 2000; received in revised form 22 February 2001; accepted 22 February 2001

Abstract

Binary blends of ethylene–styrene copolymers were studied over the full range of copolymer styrene content. A miscibility and cocrystallization map was determined from morphology as imaged with atomic force microscopy (AFM), glass transition behavior primarily from dynamic mechanical thermal analysis (DMTA), and melting behavior from differential scanning calorimetry (DSC). A difference in styrene content of about 9 wt% marked a transition from miscible to immiscible amorphous copolymer blends. The miscibility–immiscibility boundary encompassed a very small region, estimated as 9–10 wt% difference in styrene content, where partial miscibility was clearly evident. Blends in this region were characterized by an upper critical solution temperature (UCST). The phase behavior in the partial miscibility region was strongly dependent on temperature and molecular weight. The critical composition difference for blends of amorphous copolymers of about 9 wt% also applied to blends of semicrystalline copolymers. Cocrystallization of miscible, semicrystalline copolymers occurred if the styrene content difference was less than about 4 wt%. If the styrene content difference was between 4 and 9 wt%, partial cocrystallization was possible depending on the composition of the blend (wt/wt) and the thermal history of the blend.

Keywords: Ethylene–styrene copolymers; Miscibility; Blends

1. Introduction

Recent developments in catalyst technology allow for the copolymerization of ethylene with large amounts of styrene [1]. These copolymers present a broad range of structure and properties [1]. A composition of about 50 wt% styrene marks a transition from semicrystalline to amorphous copolymers. Because the span in glass transition temperature encompasses ambient temperature, differentiation is also made between amorphous copolymers that are above and below the glass transition temperature. Consequently, three distinct performance regimes are identified: semicrystalline (less than 50 wt% styrene), rubbery amorphous (50–70 wt% styrene), and glassy amorphous (70–80 wt% styrene).

Blending ethylene–styrene (ES) copolymers of different styrene content can be the basis for expanding the property spectrum. This requires an understanding of the effect of styrene content and molecular weight on miscibility and phase behavior. Furthermore, the copolymers made by this technology are statistically more uniform in microstructure and narrower in molecular weight distribution than copolymers made by conventional catalysts. Therefore, they offer an excellent model system for studying the structure-property relationships of ethylene copolymers [2,3,4] and miscibility behavior of ethylene copolymer blends [5].

Discussions of polymer miscibility usually start with the Flory–Huggins equation for the free energy of mixing of a binary blend

$$\frac{\Delta G_m}{RT} = \frac{\phi_1}{N_1}\ln\phi_1 + \frac{\phi_2}{N_2}\ln\phi_2 + \chi\phi_1\phi_2, \quad (1)$$

where ϕ_1 and ϕ_2 are the volume fractions of constituents 1 and 2, N_1 and N_2 the respective degrees of polymerization, and χ is the Flory–Huggins interaction parameter. The critical miscibility conditions are obtained by setting the derivatives of Eq. (1) equal to zero [6]. For the interaction parameter, the critical condition is

$$\chi_c = \frac{1}{2}\left[\frac{1}{\sqrt{N_1}} + \frac{1}{\sqrt{N_2}}\right]^2. \quad (2)$$

The interaction parameter for a blend of copolymers can be represented by a linear combination of the individual interaction parameters. For a mixture of two random copolymers of the same comonomers with copolymer compositions x and y, the interaction parameter is given

* Corresponding author. Tel.: +1-216-368-4186; fax: +1-216-368-6329.
E-mail address: pah6@po.cwry.edu (A. Hiltner).

0032-3861/01/$ - see front matter
PII: S0032-3861(01)00212-9

by [7,8]

$$\chi = \chi_{AB}(x - y)^2, \tag{3}$$

where χ_{AB} is the segmental interaction parameter of the comonomer units A and B. For a blend of two AB copolymers to be miscible at any concentration, χ should be less than χ_c. Combination of Eqs. (2) and (3) leads to an expression for the critical composition difference for miscibility

$$|x - y|_c = \left[\frac{1}{\sqrt{N_1}} + \frac{1}{\sqrt{N_2}}\right]\left[\frac{1}{\sqrt{2\chi_{AB}}}\right]. \tag{4}$$

According to Eq. (4), miscibility depends on comonomer content difference, but not on comonomer content per se. This has been experimentally demonstrated in some instances [9,10,11]. However, numerous exceptions, in which the critical composition difference is a function of comonomer content, are interpreted in terms of sequence distribution effects or other microstructural effects on χ_{AB} [12,13,14,15].

Varying the temperature of a binary blend also changes the interaction parameter. Usually χ decreases as the temperature is raised according to the relationship

$$\chi(T) = A + \frac{B}{T}, \tag{5}$$

where A and B are constants. If the copolymer content difference is close to $|x - y|_c$ in Eq. (4), classical upper critical solution temperature (UCST) behavior is possible, and indeed UCST behavior has been reported for some binary blends close to the critical composition difference [10,15,16].

The ES copolymers, with a broad range in comonomer content and well-characterized composition and molecular weight, provide a model system for testing Eq. (4) and related concepts of copolymer miscibility. With the assumption that the interaction parameter is purely enthalpic, χ_{AB} can be written in terms of the solubility parameter difference as:

$$\chi_{AB} = \frac{V_{ref}}{RT}(\delta_{PA} - \delta_{PB})^2, \tag{6}$$

where δ_{PA} and δ_{PB} are the solubility parameters of homopolymers A and B, and $V_{ref} = (V_A V_B)^{1/2}$ is the reference volume with V_A and V_B defined as the molar volumes of A and B units, respectively. The combination of Eqs. (4) and (6) provides an estimate of the critical composition difference. This approach was used to predict miscibility of binary ES copolymer blends [5]. From the solubility parameters of polyethylene and polystyrene, the value of χ_{ES} was estimated to be about 0.13. Using this value of χ_{ES}, the critical composition difference in styrene for copolymers with M_w of 10^5 was calculated to be about 10 wt%. This condition was validated experimentally by thermal analysis for blends of amorphous copolymers.

The present study will test the miscibility condition for binary blends of ES copolymers including semicrystalline copolymers with low styrene content. Blend morphology will be examined using atomic force microscopy (AFM) to image domains of the chemically similar components. The power of the AFM technique will be exploited to probe the compositional region of partial miscibility for the effects of temperature and molecular weight. The results will be compared with more conventional experimental methods that infer miscibility from glass transition behavior. Blends of miscible semicrystalline copolymers have the added possibility of cocrystallization [17,18,19]. The segregation scale of cocrystallization is much smaller than the micron scale of melt (liquid–liquid) phase separation [20]. Thermal analysis will be used to probe for the maximum styrene content difference that permits cocrystallization.

Table 1
Ethylene–styrene copolymers

Designation	Styrene in copolymer (wt%)	Styrene in copolymer (mol%)	aPS (wt%)	T_g or (T_β) (°C) (DMTA, 1 Hz)	M_w (kg mol^{-1})	M_w/M_n
ES4	4.3	1.2	0.1	(46)	175	2.1
ES8	8.6	2.5	0.0	(12)	171	2.1
ES13	13.1	3.9	0.0	(3)	166	2.1
ES16	15.7	4.8	0.5	N/A	N/A	N/A
ES21	21.6	6.9	0.0	(−4)	179	2.0
ES24	23.7	7.7	0.5	N/A	N/A	N/A
ES30	30.3	10.5	0.5	(−4)	177	3.7
ES35	35.1	12.7	0.2	(−9)	196	3.1
ES40	40.1	15.3	0.4	(−9)	207	4.4
ES52	51.8	22.4	1.5	−2	215	2.3
ES58(120)	57.6	26.8	0.6	8	120	2.2
ES58	57.1	26.4	0.5	8	224	1.9
ES60	59.5	28.3	0.5	10	227	2.4
ES61	61.4	30.0	0.4	14	242	3.5
ES68	67.7	36.1	0.7	23	243	1.8
ES71	70.9	39.6	0.5	29	240	6.3

The results will be the basis for establishing a miscibility and cocrystallization map based on styrene content difference.

2. Experimental

The ES copolymers described in Table 1 were synthesized by INSITE™ technology (INSITE™ is a trademark of The Dow Chemical Company). Data on the copolymer styrene content, the small amount of atactic polystyrene (aPS) present as an impurity, and molecular weight were provided by Dow. The copolymers used in this study had substantially random incorporation of styrene except that successive head-to-tail styrene chain insertions were shown by ^{13}C-NMR analysis to be absent, even with high levels of styrene incorporation. For this reason, the copolymers have been described as 'pseudorandom' ES interpolymers [1]. The copolymers are designated by the prefix ES, followed by the weight percent styrene. The weight average molecular weight (M_w) was generally in the range from 200,000 to 250,000 g mol^{-1} and the polydispersity was less than 2.5.

The copolymers were solution blended. Amorphous copolymers were dissolved in refluxing tetrahydrofuran, precipitated with water and vacuum dried at ambient temperature. Semicrystalline copolymers were dissolved in xylene at about 120°C, precipitated with cold methanol and vacuum dried at 50°C. Unless indicated otherwise, the blends were 50/50 (wt/wt) composition. Blends were compression molded into 1.3 mm thick plaques. The dried blends were heated at 190°C, pressed at 4 MPa for 15 min, and slowly cooled at about 25°C min^{-1} or quenched into a mixture of dry ice and ethanol.

Dynamic mechanical thermal analysis (DMTA) was performed on specimens cut from the plaques, with a DMTA MkII unit from Polymer Laboratories operating in the tensile mode. The relaxation spectrum was scanned from −50°C through the glass transition temperature with a frequency of 1 Hz and heating rate of 3°C min^{-1}.

Specimens with a controlled thermal history were prepared in the Rheometrics differential scanning calorimeter (DSC). Specimen pans containing approximately 15 mg specimens were heated into the melt, held at the desired temperature for 25 min or the time indicated, and either slowly cooled at 10°C min^{-1} or quenched into a mixture of dry ice and ethanol.

Heating and cooling thermograms were recorded with a Perkin–Elmer Model 7 DSC with approximately 5 mg specimens using a heating/cooling rate of 10°C min^{-1} unless otherwise indicated. Crystallinity calculations were based on a heat of fusion of 290 J g^{-1} for the polyethylene crystal.

AFM was performed on microtomed surfaces with a Digital Laboratories Nanoscope IIIa with MultiMode head and J-scanner. The tapping mode was used at ambient conditions. Commercial Si probes were chosen. The resonance frequencies of these probes were in the 300 kHz range. Height and phase images were recorded simultaneously. Because of the proximity of the glass transition to ambient temperature, the modulus difference between amorphous ES copolymers that varied only slightly in styrene content was large enough to provide good contrast in AFM phase images.

3. Results and discussion

3.1. Blends of amorphous copolymers: effect of styrene content

A styrene content difference of 6 wt% was achieved by blending ES52 and ES58. The dynamic mechanical relaxation

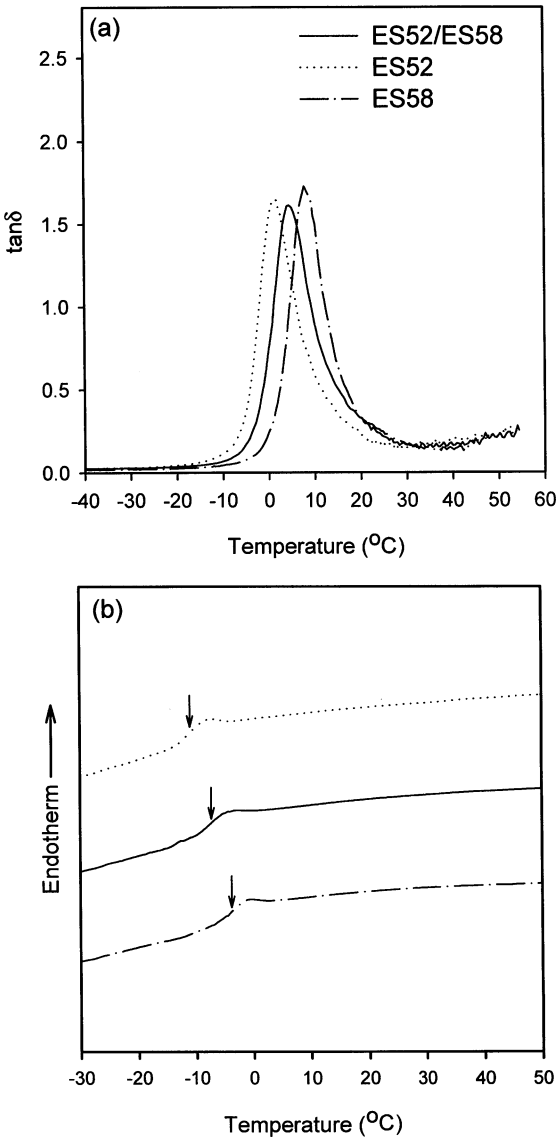

Fig. 1. Glass transition of ES52/ES58 (50/50, wt/wt) blend and blend constituents: (a) DMTA tan δ curves; (b) DSC thermograms. DMTA specimens cooled at 25°C min^{-1}, DSC specimens cooled at 10°C min^{-1}.

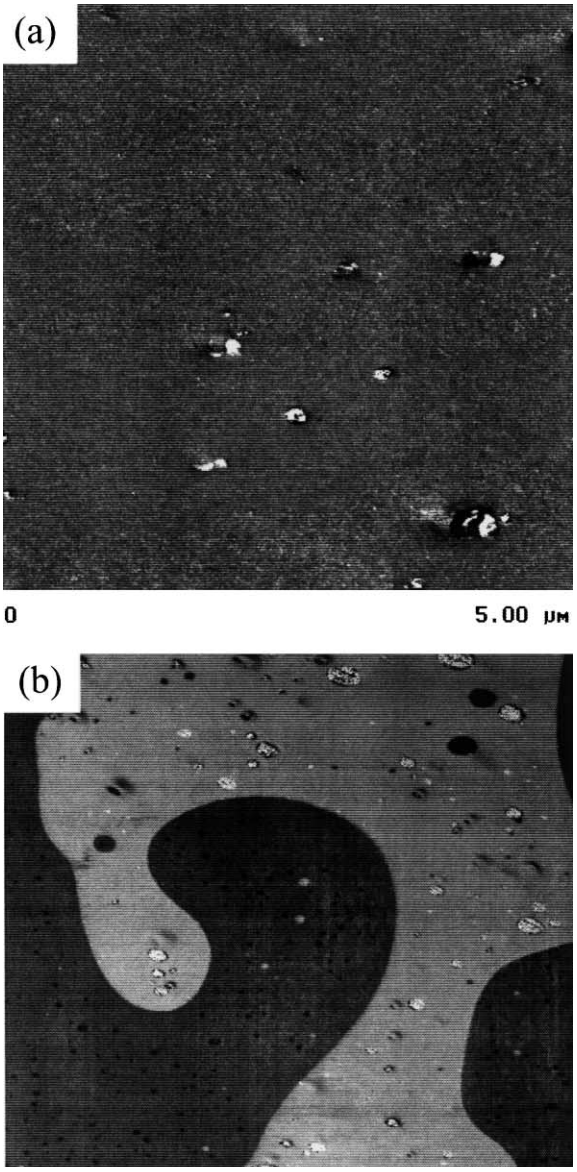

Fig. 2. AFM phase images: (a) ES52/ES58 (50/50, wt/wt) blend; (b) ES60/ES71 (50/50, wt/wt). Specimens cooled at 10°C min^{-1}.

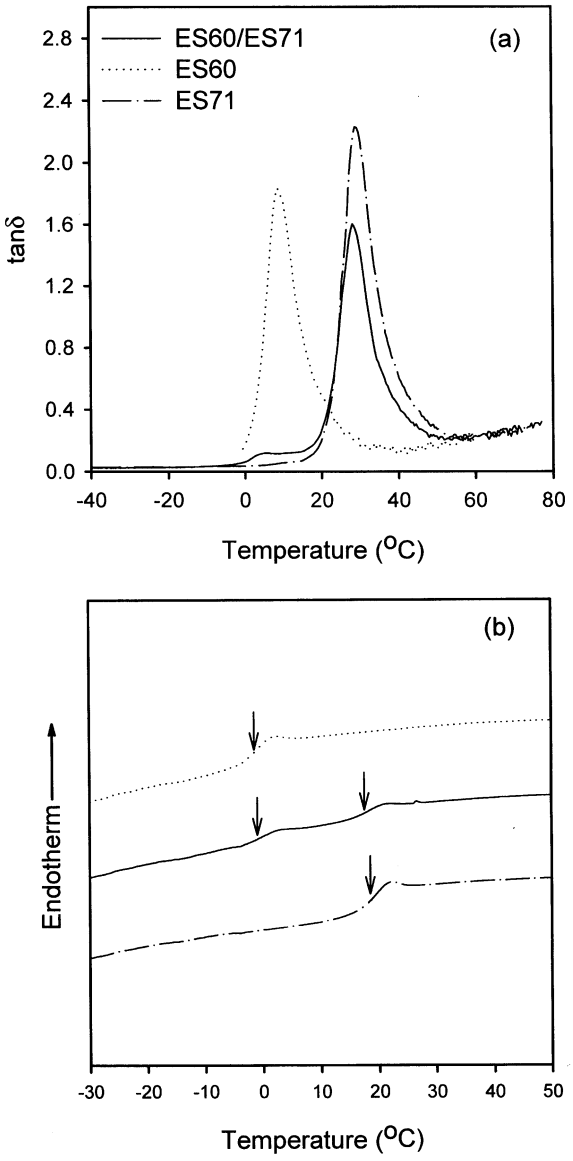

Fig. 3. Glass transition of ES60/ES71 (50/50, wt/wt) blend and blend constituents: (a) DMTA tan δ curves; (b) DSC thermograms. DMTA specimens cooled at 25°C min^{-1}, DSC specimens cooled at 10°C min^{-1}.

behavior of an ES52/ES58 (50/50, wt/wt) blend showed a single T_g at a temperature that was intermediate between the T_gs of the two constituents, Fig. 1(a). The tan δ peak of the blend had the same shape and intensity as the tan δ peaks of the constituents. The DSC thermogram of the blend also exhibited a single T_g with the same shape as the T_gs of the constituents, Fig. 1(b). Miscibility of ES52/ES58 blends, indicated by the T_g behavior, was confirmed by the appearance of a single phase in the AFM phase image, Fig. 2(a). The bright spots were harder atactic polystyrene (aPS) particles that were present as an impurity.

The styrene content difference was increased to 11 wt% by blending ES60 with ES71. The DMTA tan δ curve of the 50/50 (wt/wt) blend had two peaks, Fig. 3(a). The higher temperature peak was at almost the same temperature as the peak of ES71. The lower temperature peak was close in temperature to the ES60 peak although the intensity was much less than the intensity of the higher temperature peak. If the blend maintained a high storage modulus at temperatures where ES60 became rubbery, tan δ, which is the ratio of the loss modulus to the storage modulus, could have been small. The DSC thermogram of the ES60/ES71 blend confirmed that the constituents were almost immiscible by exhibiting two T_gs that corresponded to the T_gs of the constituents, Fig. 3(b).

The AFM phase image of the ES60/ES71 blend exhibited two phases, Fig. 2(b). The bright phase was the higher modulus ES71 and the darker phase was the lower modulus ES60. The bright aPS particles tended to concentrate in the phase with the higher styrene content. The large phase size, on the scale of tens of microns, and the sharp phase

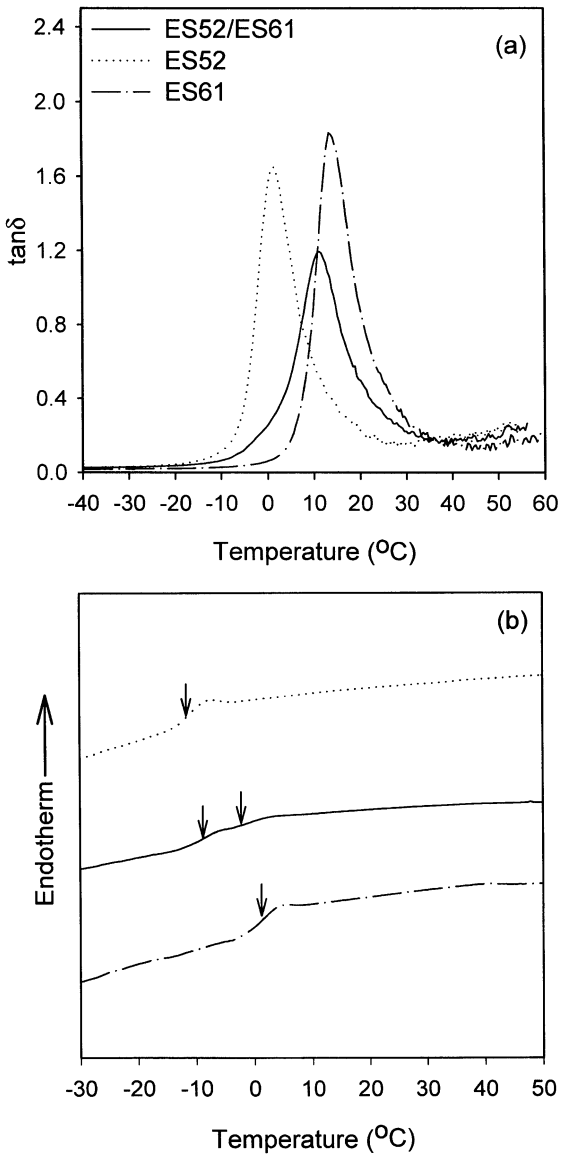

Fig. 4. Glass transition of ES52/ES61 (50/50, wt/wt) blend and blend constituents: (a) DMTA tan δ curves; (b) DSC thermograms. DMTA specimens cooled at 25°C min^{-1}, DSC specimens cooled at 10°C min^{-1}.

boundaries conclusively demonstrated the immiscibility of ES60/ES71.

A styrene content difference of 9 wt% was obtained by blending ES52 with ES61. The dynamic mechanical relaxation behavior of the 50/50 (wt/wt) blend showed a single tan δ peak at a temperature intermediate between the tan δ peaks of the constituents, Fig. 4(a). However, the peak was broader and the intensity was lower compared to the constituent tan δ peaks. The DSC thermogram of this blend exhibited a broad T_g region that encompassed two T_gs in close proximity, Fig. 4(b). The lower T_g was higher than the T_g of ES52 and the higher T_g was lower than the T_g of ES61. This blend appeared to be partially miscible with two phases, an ES52-rich phase and an ES61-rich phase.

The existence of two phases was confirmed in AFM images, Fig. 5. The brighter phase was the higher modulus ES61-rich phase, the darker phase was the lower modulus ES52-rich phase. Typically, the aPS particles concentrated in the higher styrene ES61-rich phase. The images were consistent with partially miscibility. The phase size was much smaller, on the scale of microns, and the phase boundaries more diffuse than in the immiscible ES60/ES71 blend (compare Fig. 5 with Fig. 2(b)). Generally, the interfacial tension and thus the phase size decrease as blend constituents become more miscible. The results suggested that the critical composition difference for amorphous ES copolymers with weight average molecular weight of approximately 200,000 g mol^{-1} was a styrene content difference of about 9 wt%. This confirmed the previous prediction based on solubility considerations [5].

3.2. Blends of partially miscible amorphous copolymers: effect of molecular weight and temperature

The characteristics of partial miscibility were examined by blending ES68 with ES58 of about the same molecular weight and with ES58(120) of lower molecular weight. With 10 wt% difference in styrene content, these blends were close to the miscibility condition. The 50/50 (wt/wt) blend with higher molecular weight ES58 clearly exhibited phase separation with two T_gs in DMTA curves, Fig. 6. The T_g of the ES58-rich phase appeared as a small peak at a temperature that corresponded closely to the T_g of ES58. The T_g of the ES68-rich phase appeared as a much stronger tan δ peak at a temperature several degrees lower than the T_g of ES68.

Thermograms of blends that had been slowly cooled from the melt confirmed two glass transitions temperatures that were close to the T_gs of the constituents, at -2°C for ES58 and at 11°C for ES68, Fig. 7. Quenching instead of cooling slowly, in order to retain as much as possible the phase condition at 190°C, did not alter the thermogram of the ES58 blend indicating that increasing temperature did not appreciably change the phase composition.

The tan δ curve of the 50/50 (wt/wt) blend of ES68 with the lower molecular weight ES58(120) closely resembled that of the blend with higher molecular weight ES58, Fig. 6, although the intense peak of the ES68-rich phase was shifted several degrees lower, suggesting that the slowly cooled blend with ES58(120) was slightly more miscible. The DSC thermogram of the slowly cooled blend confirmed two distinct T_gs, Fig. 7. However if the blend with lower molecular weight ES58(120) was quenched from 190°C, the two T_gs in the thermogram shifted closer together. This suggested that the blend with lower molecular weight ES58(120) was considerably more miscible at 190°C than it was at the solidification temperature when slowly cooled, which would have been considerably lower than 190°C.

The AFM images of both blends slowly cooled from 190°C exhibited phase separation on the micron size scale, Fig. 8(a),(b). However the large domains of the blend with

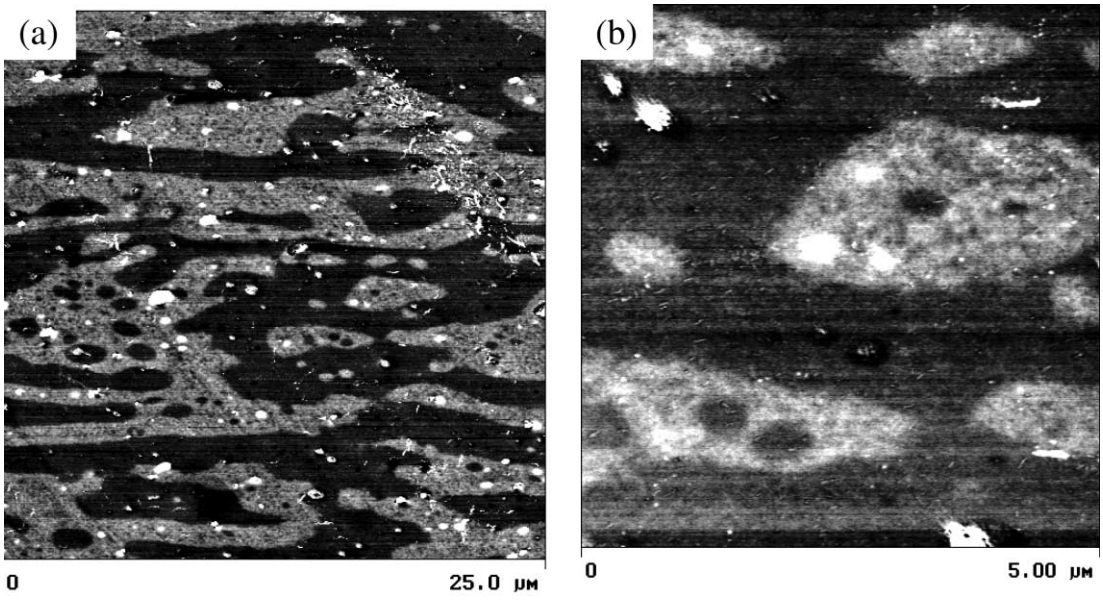

Fig. 5. AFM phase images of ES52/ES61 (50/50, wt/wt): (a) lower magnification; (b) higher magnification. Specimens cooled at 25°C min^{-1}.

the ES58(120) contained many small domains of the other phase. This 'composite' domain morphology was not present in the blend with ES58. Recalling that the blend with lower molecular weight ES58(120) was significantly more miscible at 190°C than at lower temperatures, it was reasonable to assume that large domains existing at 190°C underwent secondary phase separation due to the decrease in miscibility as the blend slowly cooled. This created the small domains. Small domains dispersed in the large domains suggested that phase separation occurred by a nucleation and growth mechanism [6].

Quenching the ES58(120) blend from 190°C, instead of cooling slowly, produced the morphology in Fig. 8(c). In this case, the large domains did not contain small domains. Instead, the domain morphology closely resembled that of the slowly cooled blend with higher molecular weight ES58, although the contrast between phases in AFM images was not as sharp as for the blend with higher molecular weight

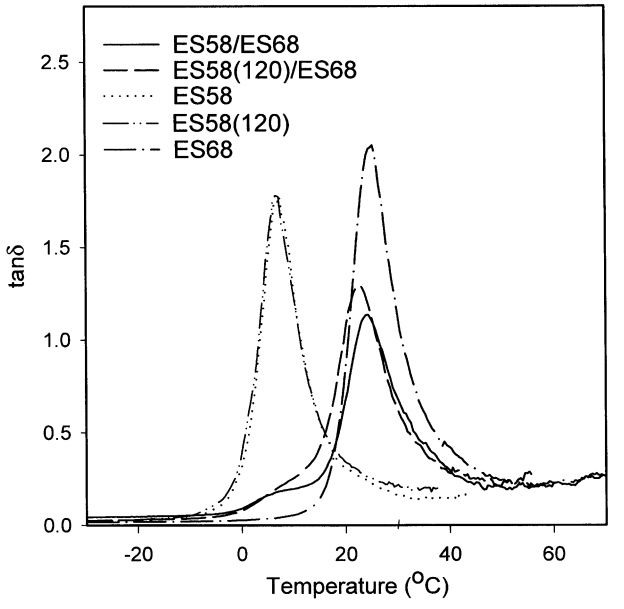

Fig. 6. DMTA tan δ curves of ES58/ES68 and ES58(120)/ES68 (50/50, wt/wt) blends and blend constituents. Specimens cooled at 25°C min^{-1}.

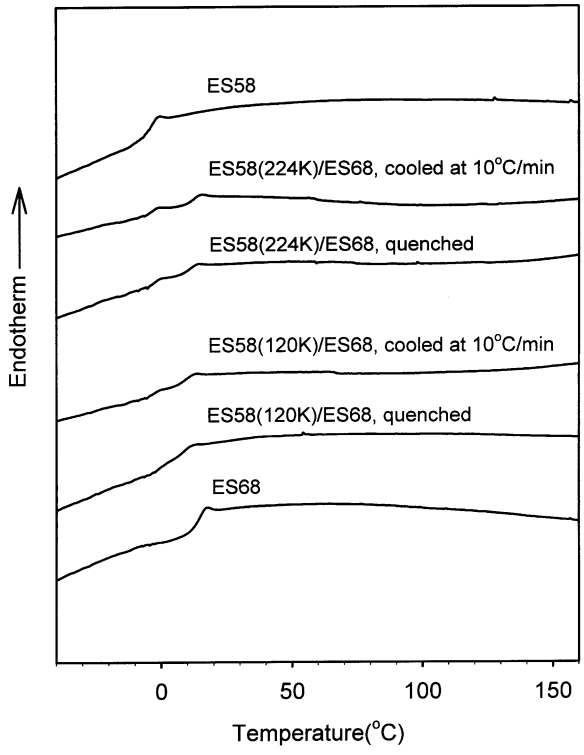

Fig. 7. Thermograms of ES58/ES68 and ES58(120)/ES68 (50/50, wt/wt) blends quenched from 190°C and cooled from 190°C at 10°C min^{-1}.

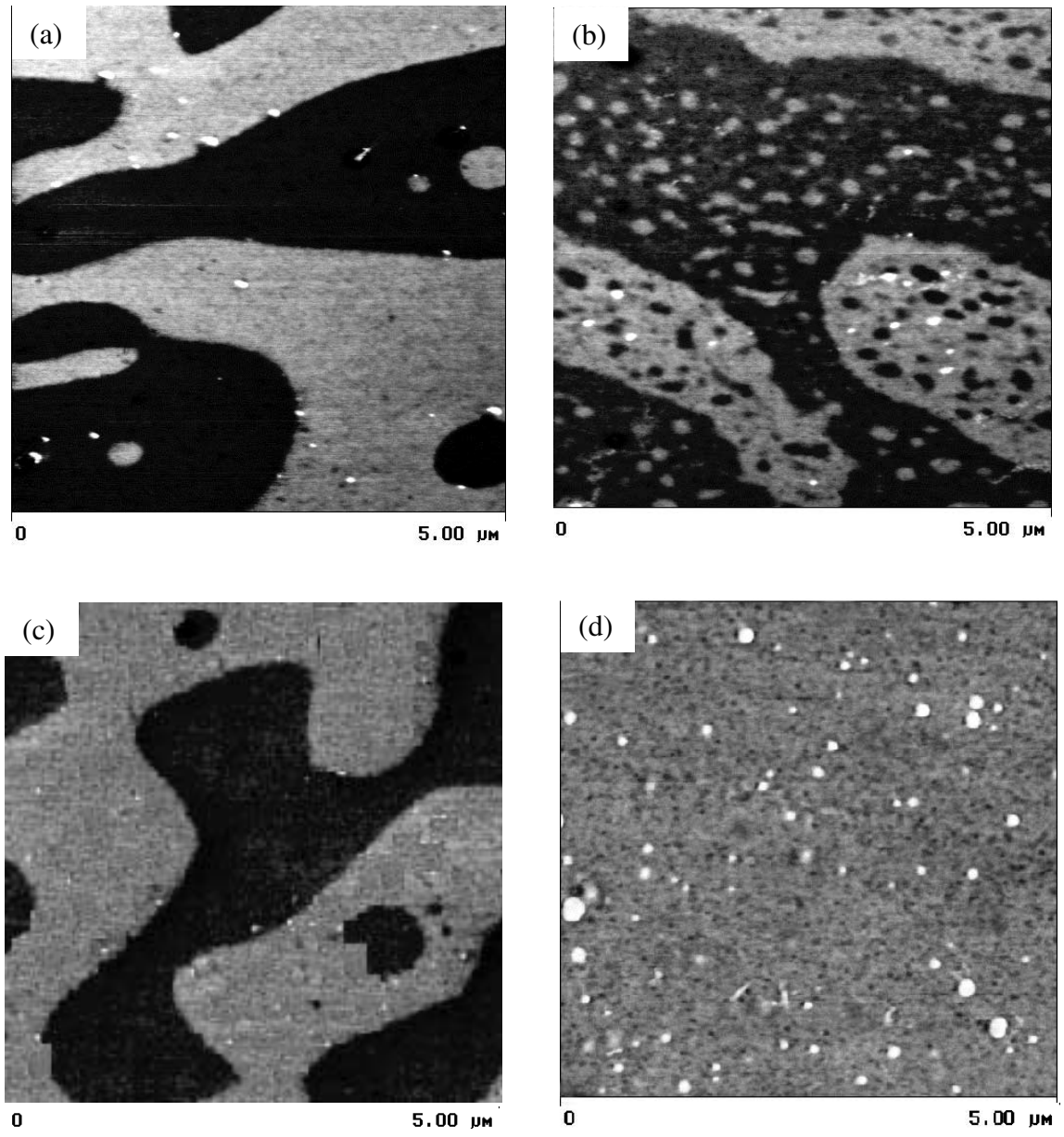

Fig. 8. AFM phase images: (a) ES58/ES68 (50/50, wt/wt) cooled from 190°C at 10°C min^{-1}; (b) ES58(120)/ES68 (50/50, wt/wt) cooled from 190°C at 10°C min^{-1}; (c) quenched from 190°C; (d) quenched from 250°C.

ES58. Because the modulus difference between phases, and thus the composition difference, determined the contrast, this was further evidence that the lower molecular weight ES58(120) was much more miscible with ES68 than the higher molecular weight ES58 at 190°C.

In addition to having lower molecular weight than ES58, ES58(120) also contained 0.5 wt% more styrene than ES58, and thus was closer in composition to ES68. Because the smaller composition difference promoted higher miscibility of ES58(120) with ES68, the relative effects of molecular weight and styrene content difference had to be estimated before the higher miscibility of ES58(120) could be attributed primarily to a molecular weight effect. Considering that the system was close to miscible, the magnitudes of the (positive) enthalpic term and the (negative) entropic terms in Eq. (1) were about the same. From Eq. (3) with $\chi_{ES} = 0.13$, the smaller composition difference decreased the enthalpic term by about 10% compared to an almost 50% decrease in the entropic contribution from the lower molecular weight.

The noticeable temperature dependence of the phase composition of the ES58(120) blend suggested that it might have a UCST. The blend was probed for disappearance of phase separation by quenching to the glassy state from elevated temperature to fix the melt morphology, and subsequently recording the thermogram to obtain the glass transition behavior. A similar approach was used to characterize melt miscibility of other blend systems consisting of

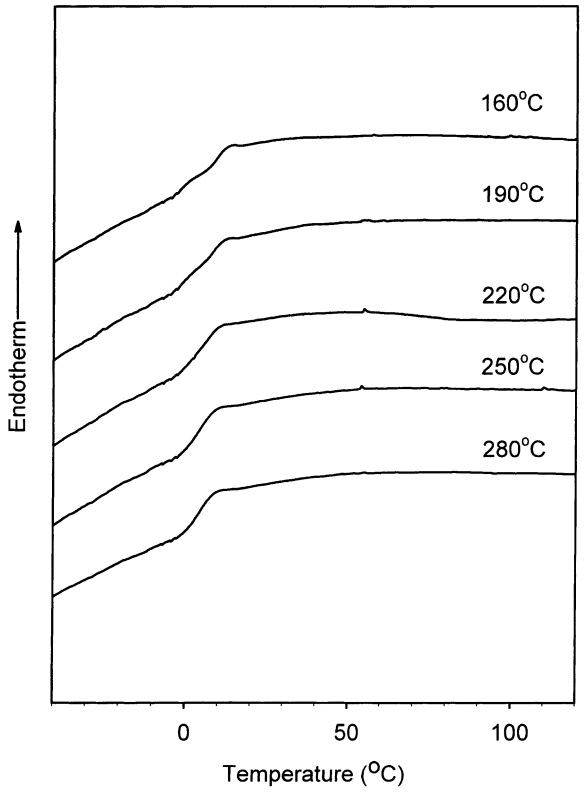

Fig. 9. Thermograms of ES58(120)/ES68 (50/50, wt/wt) after quenching from various temperatures.

chemically similar components [16,21,22]. Thermograms of 50/50 (wt/wt) blends quenched from various temperatures are shown in Fig. 9. The blend quenched from the lowest temperature, 160°C, clearly exhibited two T_gs. As the melt temperature increased, the gradual shift of the T_gs closer together indicated that the blend became more miscible. At 220°C, two T_gs were almost indistinguishable, and at 250°C the two T_gs merged into a single sharp glass transition indicating that the blend formed a single phase. Existence of a UCST in ES58(120)/ES68 blends was confirmed by the AFM image of the blend quenched from 250°C in Fig. 8(d). This showed a homogeneous texture except for the bright particles of atactic polystyrene.

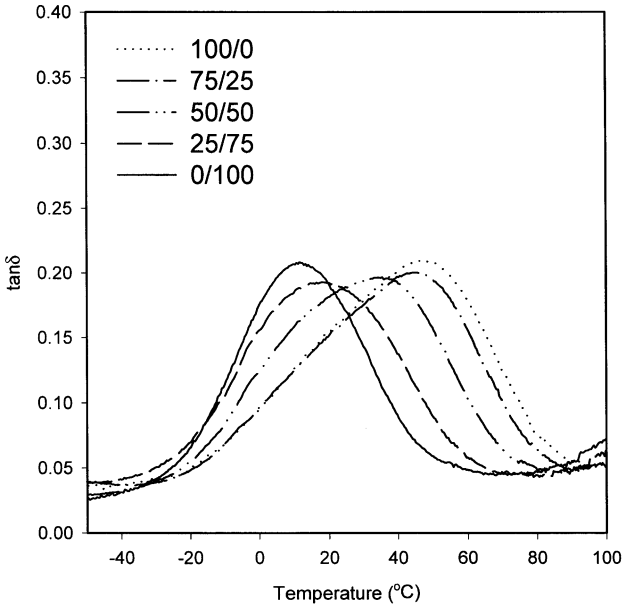

Fig. 10. DMTA tan δ curves of ES4/ES8 blends and blend constituents. Specimens quenched from 190°C.

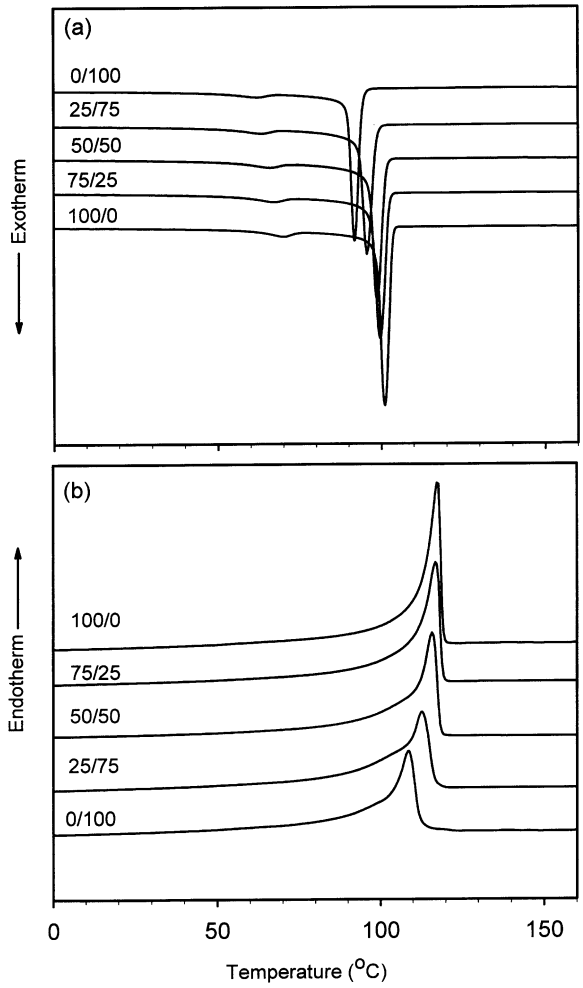

Fig. 11. DSC thermograms of ES4/ES8 blends and blend constituents: (a) cooling at 10°C min^{-1}; (b) subsequent heating at 10°C min^{-1}.

3.3. Blends of semicrystalline copolymers

The condition for ambient temperature miscibility established for amorphous copolymer blends, about 9 wt% styrene content difference, was tested for blends of semicrystalline copolymers. For this purpose, results for blends that differed in styrene content by 4, 9 and 17 wt% are presented in detail. Blends of miscible semicrystalline copolymers possessed the additional possibility for cocrystallization of ethylene-rich chain segments. Thus, if blends were

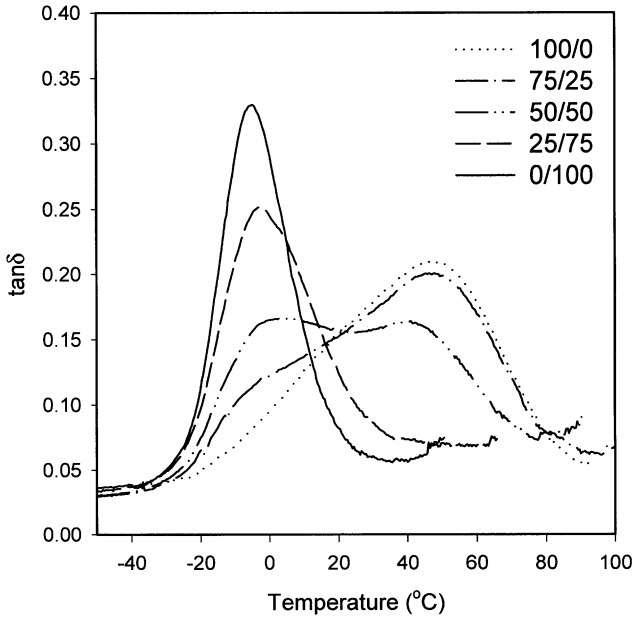

Fig. 12. DMTA tan δ curves of ES4/ES21 blends and blend constituents. Specimens quenched from 190°C.

miscible, they were also examined at a smaller size scale for crystallization habit.

Experiments on blends of semicrystalline copolymers focused on miscibility in the melt by quenching from 190°C. The tan δ curves of ES4, ES8 and their blends are shown in Fig. 10. The quenched semicrystalline copolymers typically exhibited a broad β-relaxation, accompanied by a large modulus drop, that corresponded to the glass transition of the amorphous regions. The breadth of the peak, and the increase in T_β with crystallinity, were attributed to constraints imposed by the presence of a crystalline phase. The crystalline α-relaxation was not observed in quenched specimens, it only became prominent in slowly cooled specimens with improved crystalline order. The ES4/ES8 blends exhibited a single β-relaxation at a temperature intermediate between the β-relaxations of ES4 at 47°C and ES8 at 18°C. Although the peak for the quenched blends was somewhat broader and slightly less intense than that of the constituents, the presence of a single peak was taken as evidence of the miscibility expected for blends that differed in styrene content by only 4 wt%.

Single crystallization and melting peaks in DSC thermograms of ES4/ES8 blends confirmed this important characteristic of an isomorphic system, Fig. 11. Gradual progression of the shape of the melting and crystallization peaks with blend composition was taken as an indication of cocrystallization. Additivity of the melting enthalpy based on constituent weight fractions further indicated that ES4 and ES8 cocrystallized from a miscible melt [17,18].

The tan δ curves of ES4, ES21 and their blends with a 17 wt% difference in styrene content are shown in Fig. 12. The ES4/ES21 50/50 (wt/wt) and 75/25 (wt/wt) blends had two well-separated β-relaxation peaks at temperatures approximately corresponding to the temperatures of the constituent β-relaxations at −4°C for ES21 and 47°C for ES4. The intensity of the peaks varied according to composition. A peak for an ES4-rich phase was not distinguishable in the 25/75 (wt/wt) blend, probably because it was covered by the tail of the lower temperature relaxation peak. Because the blends were quenched, the dynamic mechanical relaxation behavior reflected the phase condition in the melt state. Two relaxation peaks indicated that the blends were not miscible, as expected from the styrene content difference of 17 wt%.

The phase behavior of ES4/ES21 blends was confirmed by probing the morphology of blends quenched from the melt into a dry ice–ethanol mixture. Fig. 13(a) shows the

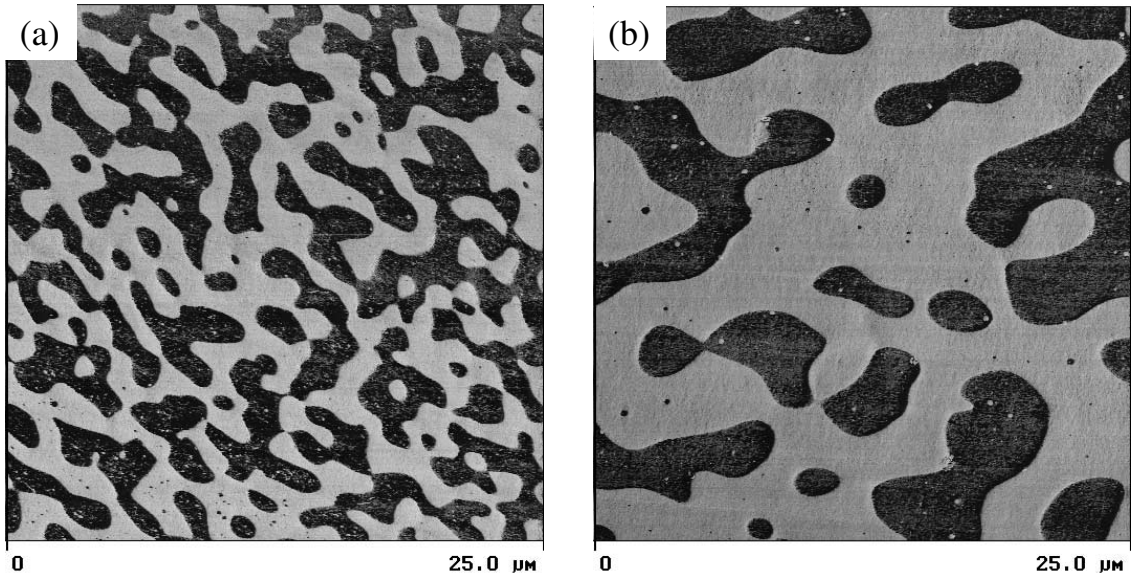

Fig. 13. AFM phase images of ES4/ES21 (50/50, wt/wt) blend: (a) after 20 min at 190°C; (b) after 2 h at 190°C. Specimens quenched from 190°C.

AFM image of the quenched blend after it was taken to 190°C for 20 min. The two-phase morphology is evident. The darker phase is the ES21-rich phase with a lower modulus, and the lighter phase is the ES4-rich phase with a higher modulus. Phase separation in the melt at 190°C was confirmed by the appearance of phase coarsening after the melt was held at 190°C for 2 h, Fig. 13(b).

Crystallization thermograms of ES4/ES21 blends exhibited two peaks, Fig. 14(a). For the 75/25 and 50/50 (wt/wt) blends, the exothermic peak temperatures corresponded to the crystallization peaks of the constituents. For the 25/75 blend, a 10°C decrease in crystallization temperature of ES4 was observed. Depression in the crystallization temperature of the minor, higher melting constituent was previously reported in blends of other ethylene copolymers [23]. In this case, the phenomenon was attributed to amplification of interfacial effects in the small domains of the biphasic melt. The subsequent melting thermograms of ES4/ES21 blends, shown in Fig. 14(b), exhibited two distinct melting peaks corresponding to the melting temperatures of the constituents. Moreover, the experimental melting thermograms coincided with thermograms calculated by linear addition of the constituent thermograms. The crystallization

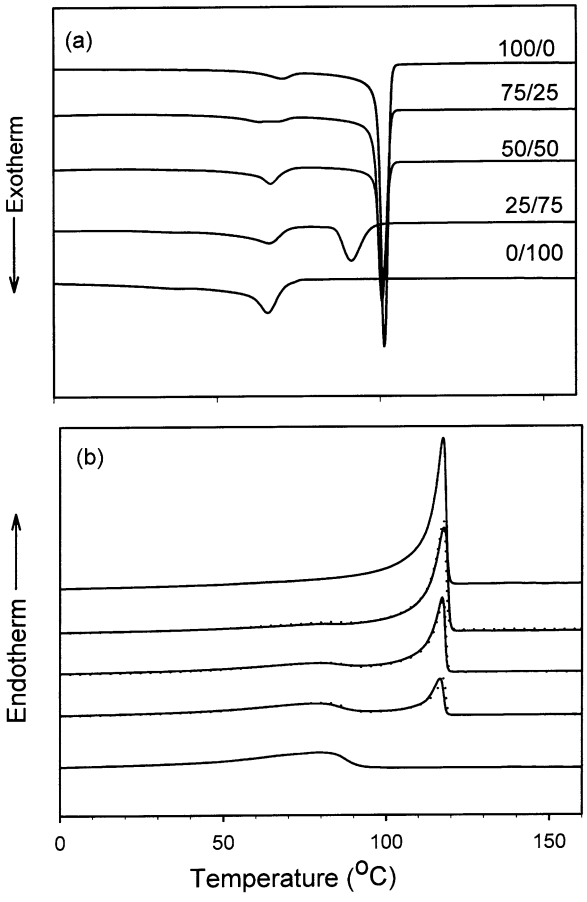

Fig. 14. DSC thermograms of ES4/ES21 blends and blend constituents: (a) cooling at 10°C min^{-1}; (b) subsequent heating at 10°C min^{-1}. The dotted line was calculated from the weighted constituent contributions.

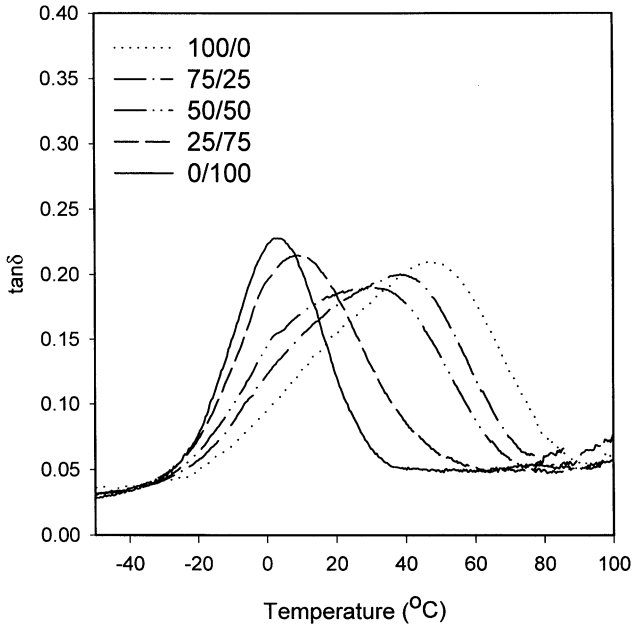

Fig. 15. DMTA tan δ curves of ES4/ES13 blends and blend constituents. Specimens quenched from 190°C.

and melting behavior indicated that the constituents crystallized independently as separate crystal populations, which was totally consistent with immiscibility in the melt.

A styrene content difference of 9 wt% was obtained by blending ES4 with ES13. The tan δ curves of the blends exhibited a single β-relaxation peak at a temperature intermediate between the β-transition temperatures of the constituents, Fig. 15. However, the blend peaks were generally

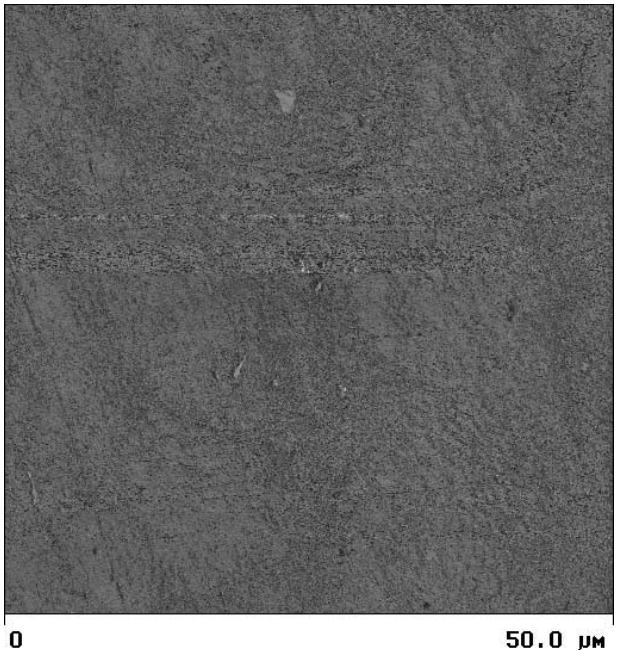

Fig. 16. AFM phase image of ES4/ES13 (50/50, wt/wt) cooled at 1°C min^{-1} from 190°C.

broader and less intense than the constituent peaks. The effect of blending on the β-relaxation was similar to that observed with miscible ES4/ES8 blends (compare Fig. 15 with Fig. 10.) In contrast to blends of amorphous copolymers, it was difficult to draw definitive conclusions regarding miscibility of semicrystalline copolymers from the shape of the β-relaxation peak. However, the AFM phase image of the slowly cooled blend clearly exhibited a single phase to indicate that ES4 and ES13 were miscible, Fig. 16.

The ES4/ES13 blends, being miscible in the melt, possessed the additional possibility for cocrystallization. Thermograms of quenched ES4/ES13 75/25 and 50/50 (wt/wt) blends exhibited a single melting peak whereas the 25/75 blend had a double melting peak, Fig. 17(a). The thermogram of the 75/25 blend was not affected by cooling rate. However, with decreasing cooling rate, a second, lower temperature melting peak appeared in the thermogram of the 50/50 blend, and the two melting peaks of the 25/75 blend shifted further apart, closer to the melting peaks of the constituents, Fig. 17(a) and (b).

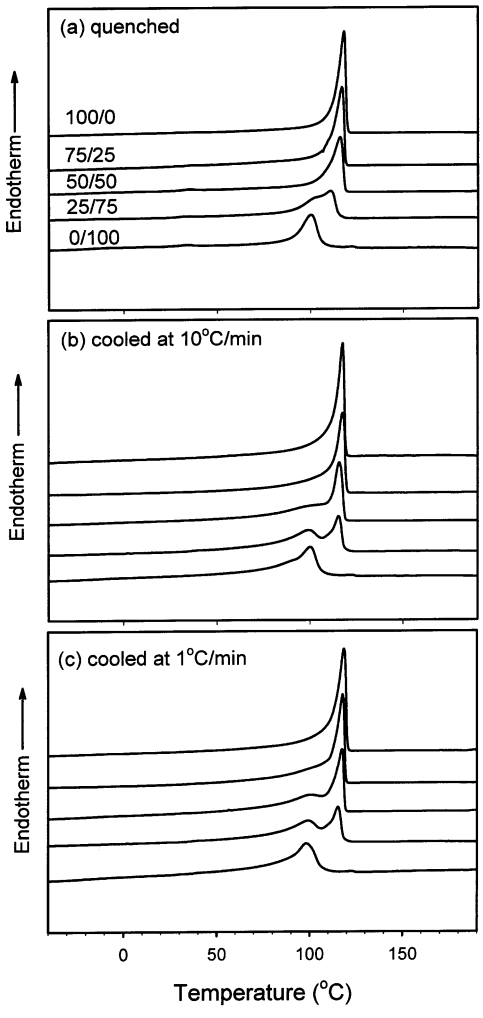

Fig. 17. DSC heating thermograms of ES4/ES13 blends and blend constituents: (a) quenched from 190°C; (b) cooled from 190°C at 10°C min^{-1}; (c) cooled from 190°C at 1°C min^{-1}.

The constituents appeared to partially cocrystallize with the extent of cocrystallization dependent upon the cooling rate. It is not unusual for the degree of cocrystallization to depend on factors that affect the diffusion process required for molecular segregation such as blend composition (wt/wt) and thermal history [24,25].

3.4. Miscibility and cocrystallization map

Miscibility and cocrystallization of binary copolymer blends was studied over the full range of styrene content using primarily AFM images of blend morphology and, where possible, DMTA and DSC results. Conventional methods for imaging domain morphology were not useful for these blends because of the similarity in chemical composition of the constituents. However the modulus differences were large enough that AFM phase images clearly revealed the domain morphology. This method was particularly valuable for characterizing blends of semicrystalline copolymers where dynamic mechanical analysis was found to be inconclusive. It should be noted that the AFM images revealed the phase behavior at somewhat different temperatures for crystalline and amorphous blends. Being quenched from the melt, the observed morphology of the crystalline blends related most closely to the 190°C melt; whereas the amorphous blends were slowly cooled and the observed morphology more closely represented the equilibrium situation at the solidification temperature which was considerably lower than 190°C. However the effect of temperature on χ over the range studied was small compared to the effect of styrene content difference, and therefore the effect of temperature was negligible except in the very small range of partial miscibility.

Based on the experimental observations, a miscibility map for binary blends was constructed. As presented in Fig. 18, open symbols indicate miscible blends and filled symbols indicate blends that phase separate. It appears that the critical styrene content difference of about 9 wt% applies to all blends of ethylene-styrene copolymers with molecular weight of approximately 200,000 g mol^{-1}. For this system, miscibility depends only on the difference in comonomer content in accordance with Eq. (4) with composition expressed as weight fraction. Because weight fraction of ES copolymers is essentially equivalent to volume fraction [4], the critical composition difference is also constant if expressed as volume fraction in accordance with other thermodynamic properties such as solubility parameter [26]. In contrast, the critical composition difference expressed as mole fraction would show considerable variation over the copolymer composition range used to construct Fig. 18. It should be noted that Eq. (3) appears not to hold for other α-olefin copolymer blends with either mole fractions or weight fractions [14]. This is attributed to an additional contribution to the interaction parameter from local packing effects, which derive from differences in chain flexibility [27]. Eq. (3) may work well for binary ES copolymer

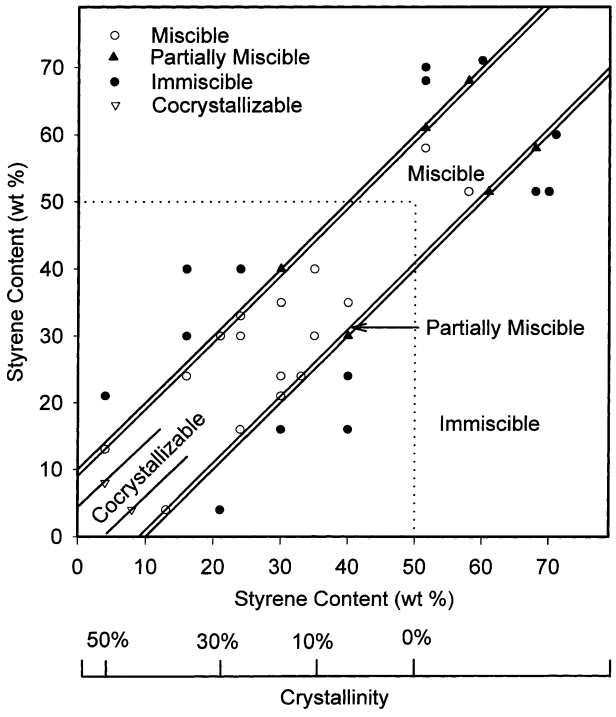

Fig. 18. Miscibility map of binary ethylene–styrene copolymer blends.

blends because the difference in chain flexibility is negligible for copolymers that differ in styrene content by only 9 wt% [4].

The transition from miscibility to immiscibility occurs over a very small change in styrene content difference. Increasing the styrene content difference from 9 to 11 wt% is sufficient to change the system from miscible to immiscible for copolymers of this molecular weight. The solid lines in Fig. 18 indicate the very small region between 9 and 10 wt% styrene content difference where partial miscibility is clearly evident. The phase composition of blends in this region shows a strong dependence on temperature and molecular weight. Some of the blends exhibit an UCST.

Blends of semicrystalline ES copolymers, with 50 wt% styrene or less, are differentiated from blends of amorphous copolymers by the dotted lines in Fig. 18. Miscible blends of semicrystalline copolymers have the added possibility of cocrystallization. The segregation scale of cocrystallization is much smaller than the micron scale of melt (liquid–liquid) phase separation. Moreover, cocrystallization depends strongly on kinetic factors of nucleation and growth. Nevertheless, it appears that cocrystallization of semicrystalline ES copolymers occurs readily if the styrene content difference is less than about 4 wt%. If the styrene content difference is higher, partial cocrystallization is possible depending on the composition of the blend (wt/wt) and the thermal history of the blend.

Acknowledgements

The authors thank Dr M.J. Guest and Dr S.P. Chum of The Dow Chemical Company for providing technical assistance. The financial support of The Dow Chemical Company is gratefully acknowledged.

References

[1] Chen H, Guest MJ, Chum S, Hiltner A, Baer E. J Appl Polym Sci 1998;70:109.
[2] Chen HY, Stepanov EV, Chum SP, Hiltner A, Baer E. J Polym Sci, Part B: Polym Phys 1999;37:2373.
[3] Chen HY, Stepanov EV, Chum SP, Hiltner A, Baer E. Macromolecules 1999;32:7587.
[4] Chen HY, Stepanov EV, Chum SP, Hiltner A, Baer E. Macromolecules 2001 (in press).
[5] Cheung YW, Guest MJ. J Polym Sci, Part B: Polym Phys 2000;38:2976.
[6] Utracki LA. Polymer alloys and blends. Munich: Hanser, 1989.
[7] Scott RL. J Polym Sci 1952;9:423.
[8] ten Brinke G, Karasz FE, MacKnight WJ. Macromolecules 1983;16:1827.
[9] Molau GE. Polym Lett 1965;3:1007.
[10] Aoki Y. Macromolecules 2000;33:6006.
[11] Chai Z, Sun R, Karasz FE. Mechanical behavior of materials IV. In: Jono M, Inoue T, editors. London: Pergamon Press, 1991.
[12] Chai Z, Sun R, Karasz FE. Macromolecules 1992;25:6113.
[13] Delfolie C, Dickinson C, Freed KF, Dudowicz J, MacKnight WJ. Macromolecules 1999;32:7781.
[14] Graessley WW, Krishnamoorti R, Balsara NP, Butera RJ, Fetters LJ, Lohse DJ, Schulz DN, Sissano JA. Macromolecules 1994;27:3896.
[15] Kohl PR, Seifert AM, Hellmann GP. J Polym Sci, Part B: Polym Phys 1990;28:1309.
[16] Ueda H, Karasz FE. Macromolecules 1985;18:2719.
[17] Alamo RG, Glaser RH, Mandelkern L. J Polym Sci, Part B: Polym Phys 1988;26:2169.
[18] Schuman T, Stepanov EV, Nazarenko S, Capaccio G, Hiltner A, Baer E. Macromolecules 1998;31:4551.
[19] Tashiro K, Stein RS, Hsu SL. Macromolecules 1992;25:1801.
[20] Wignall GD, Alamo RG, Londorno JD, Mandelkern L, Kim MH, Lin JS, Brown GM. Macromolecules 2000;33:551.
[21] Lehr MH. Polym Engng Sci 1985;25:1056.
[22] Crist B, Hill MJ. J Polym Sci, Part B: Polym Phys 1997;35:2329.
[23] Bensason S, Nazarenko S, Chum S, Hiltner A, Baer E. Polymer 1997;38:3513.
[24] Kim M-H, Alamo RG, Lin JS. Polym Engng Sci 1999;39:2117.
[25] Galante MJ, Mandelkern L, Alamo RG. Polymer 1998;39:5105.
[26] Reichart GC, Graessley WW, Register RA, Lohse DJ. Macromolecules 1998;31:7886.
[27] Fredrickson GH, Liu AJ, Bates FS. Macromolecules 1994;27:2503.